Azimuthal coherence of the sound field in the vicinity of a high performance military aircraft

Kevin M. Leete, Alan T. Wall, Kent L. Gee, Tracianne B. Neilsen, Blaine M. Harker, and Michael M. James

Citation: Proc. Mtgs. Acoust. **29**, 045007 (2016); doi: 10.1121/2.0000673
View online: https://doi.org/10.1121/2.0000673
View Table of Contents: http://asa.scitation.org/toc/pma/29/1
Published by the Acoustical Society of America

Proceedings of Meetings on Acoustics

Volume 29 http://acousticalsociety.org/

172nd Meeting of the Acoustical Society of America

Honolulu, Hawaii

28 November - 2 December 2016

Physical Acoustics: Paper 2pPA8

Azimuthal coherence of the sound field in the vicinity of a high performance military aircraft

Kevin M. Leete
Physics and Astronomy, Brigham Young University, Provo, UT, 84604; kevinmatthewleete@gmail.com

Alan T. Wall
Battlespace Acoustics Branch, U.S. Air Force Research Lab., Dayton, OH; alan.wall.4@us.af.mil

Kent L. Gee, Tracianne B. Neilsen and Blaine M. Harker
Physics and Astronomy, Brigham Young University, Provo, UT, 84604; kentgee@byu.edu, tbn@byu.edu, blaineharker@gmail.com

Michael M. James
Blue Ridge Research and Consulting LLC, Asheville, NC; michael.james@blueridgeresearch.com

Mixing noise from a jet engine originates from an extended spatial region downstream of the nozzle and is partially correlated both spatially and temporally. Previously, the coherence properties in the downstream direction of the sound field of a tethered military aircraft were investigated, resulting in the identification of different spatial regions based on coherence length [B. M. Harker et al., AIAA J. 54, 1551-1566 (2016)]. In this study, a vertical array of microphones to the side of the jet plume is used to obtain the azimuthal coherence of the sound field. Although multipath interference effects and a limited angular aperture make coherence length calculation impossible, information about upper and lower bounds can be extracted. The measured azimuthal coherence as a function of downstream distance and frequency is then compared to that predicted by sound field reconstructions using multisource, statistically-optimized near-field acoustical holography (M-SONAH) [A. T. Wall et al., J. Acoust. Soc. Am., 139, 1938-1950 (2016)]. This comparison helps to benchmark the performance of a reduced-order M-SONAH algorithm that employs only axisymmetric cylindrical basis functions to represent the sound field.

Published by the Acoustical Society of America

 https://doi.org/10.1121/2.0000673

1. INTRODUCTION

Extensive study by the jet noise community of the sound fields produced by both laboratory and full-scale jets is on-going. One aim of these studies is to propose potential equivalent source models to reproduce their unique characteristics. The prevailing theory to describe these fields was solidified by Tam[1] to show that there are at least two source mechanisms involved in the interaction between the jet plume and the ambient air: fine-scale turbulence and large-scale turbulence. Each source type produces a characteristic frequency spectrum, the large-scale spectrum (LSS) being more haystack-like around a certain frequency and fine-scale spectrum (FSS) more broadband.[2] The noise generated by the turbulent large-scale structures is more self-coherent and radiates directionally at a large aft angle (measured from the jet inlet). The noise generated by the fine-scale interactions radiates with lower amplitude[3] in an omnidirectional fashion, though it is masked by the large scale turbulent structure noise in the main radiation lobe. Since the two sources of jet noise are mutually uncorrelated and the large-scale structures are partially self-correlated, correlation and coherence in the near to mid fields at different points reflect what kind of source is dominating the radiation in that direction. It has been shown[4] that the field is more coherent in areas of maximum radiation, (where large scale structures dominate) and less coherent towards the sideline as well as downstream in the so-called "cone of silence."

One method to represent a partially correlated field is to decompose the field (or source) into orthogonal basis functions, where a superposition of mutually incoherent, but self-coherent functions add to represent the partially coherent field. This has applied to jet noise using Fourier decomposition[5], proper orthogonal decomposition[6], and various wavepacket types.[7,8,9,10,11] The choice of basis functions is arbitrary when the sole purpose is to reconstruct a field, though the eventual goal may be to compare these mathematical constructs to actual fluid dynamic phenomenon, so nonphysical shapes are discouraged. Decomposition of the jet noise field and source using a cylindrical coordinate system is convenient because it allows decomposition into axial and azimuthal modes. Considering the azimuthal modes, because they are mutually incoherent, a reduced azimuthal field coherence must be due to the mixing of two or more azimuthal modes.[6,8] Several studies have calculated both correlations and coherence in the acoustic field, and have found that azimuthal coherence decreases with increasing frequency.[8,12,13,14,15]

Most of the studies involving azimuthal variation in the jet noise field deal with laboratory-scale jets in an anechoic environment, where measurement apertures cover an extended portion of the jet plume. The current study takes data from a measurement of a high performance military aircraft[16] and calculates the azimuthal coherence as a function of downstream distance. The difficulty in calculating the coherence due to the presence of a ground reflection and a limited measurement aperture is addressed, and a parameter called the coherence angle, ϕ_{γ^2}, is introduced. Calculations of ϕ_{γ^2} illustrate similar trends in azimuthal coherence as seen in laboratory-scale jet studies. Additionally, a reconstruction of the sound field along the measurement aperture is performed using multi-source statistically optimized near-field acoustical holography[17], where the holography method is limited to the use of a single axisymmetric azimuthal mode to reconstruct the field. The difference between the reconstructed and measured fields is small for the frequencies where the azimuthal coherence over the reconstruction aperture is large.

2. EXPERIMENT AND ANALYSIS

A. Military aircraft data

The data used in this study were collected at the same measurement as in Ref 16, though with the array in a different orientation and at different positions than were analyzed in that study. A "patch and scan" method was used to generate a measurement plane approximately parallel to the shear layer of a tethered aircraft operating at afterburner. This was done by taking a 90 element, two-dimensional array of microphones and collecting data at a single location, then moving it to an adjacent location to cover the total desired aperture. The array was arranged vertically (rotated 90° from the orientation shown in Figure 2 of Ref. 16) with 5 columns of 18 rows of microphones with 0.15 m inter-element spacing. The center of the array was set to the jet centerline height ($y = 1.91$ m). Figure 1 contains a schematic of the measurement geometry, with the tethered aircraft nozzle over the origin. The z axis is the distance downstream from the nozzle, and the angle ϕ is the azimuthal angle from horizontal plane at the height of the jet centerline around the plume. The aperture of the entire measurement surface spanned from $\phi \sim \pm 10°$ (azimuthal coverage decreased with increasing z due to the array becoming further from the jet centerline) and $z = 5$ m to $z = 19$ m.

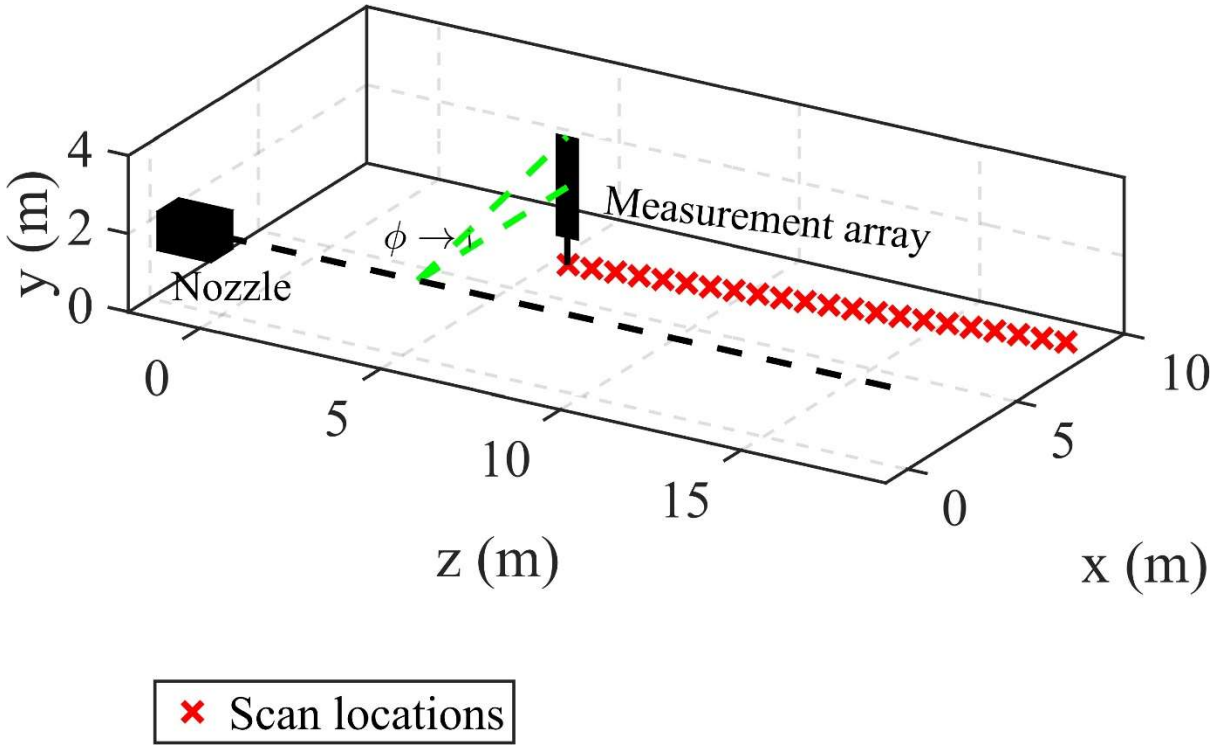

Figure 1 Schematic of test. The tethered aircraft was placed such that the nozzle (black box) was over the origin, the dashed black line represents the jet centerline that paralleled the z axis, and the angle ϕ is measured from the height of the centerline around the azimuth. The measurement array was a 18 by 5 grid of microphones with 6" spacing

Because of the patch and scan method, coherence can only be calculated between points in the same scan. Figure 2 contains the narrowband levels collected along the measurement plane for a few octave band center frequencies. The horizontal and vertical axes of the plots are the z and ϕ coordinates, with the color corresponding to the narrowband sound pressure level. The black lines show the boundaries between adjacent scans. The interference of the ground-reflected sound

creates large nulls in the measurement plane which are readily apparent in the 250 and 500 Hz cases. Above 1000 Hz, the physical spacing between the nulls was smaller than the inter-element spacing of the array so they are not well resolved. As frequency increases, the area of maximum radiation focuses to lower z values due to the frequency-dependent directivity of the source. In some instances (e.g. 500 Hz), scattering effects due to the array can be seen where levels in the middle of a patch are slightly higher than the levels at the edge of the patch. The frequency-dependent levels in the field will be used to give insight into the trends in coherence.

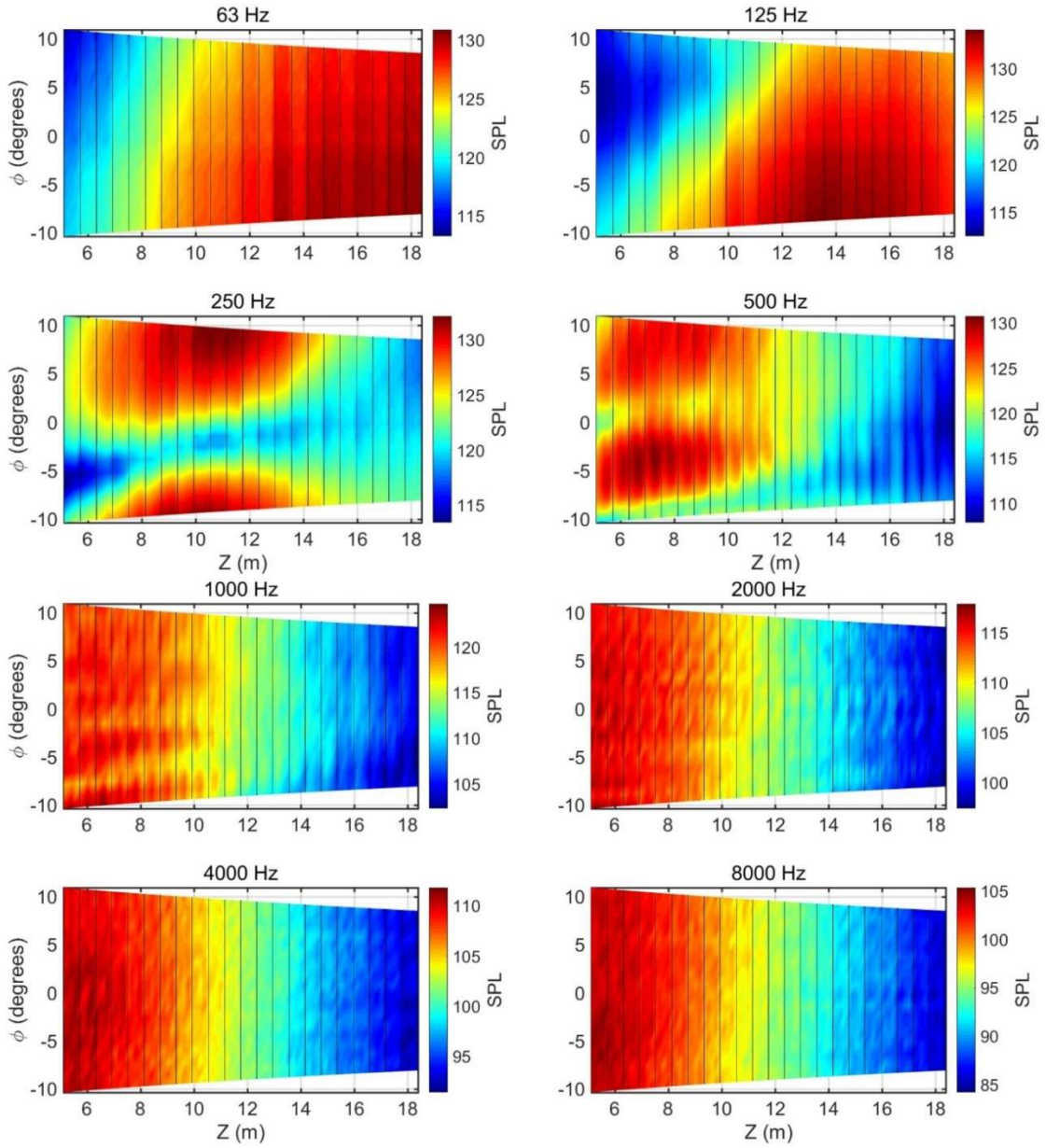

Figure 2 Sound pressure level of the jet noise field along the measurement plane as a function of downstream distance (z) and azimuthal angle (ϕ) for the octave band center frequencies between 63 and 8000 Hz. The black lines separate the 22 different array locations. The array receded from the jet centerline at larger downstream distances so the angular coverage decreased.

B. Azimuthal coherence

The coherence function, γ^2, is a frequency-dependent quantity obtained by the ratio of the magnitude squared of the cross spectrum between two arbitrary signals x and y and the product of their autospectra:

$$\gamma^2 = \frac{|G_{xy}|^2}{G_{xx}G_{yy}}. \quad (1)$$

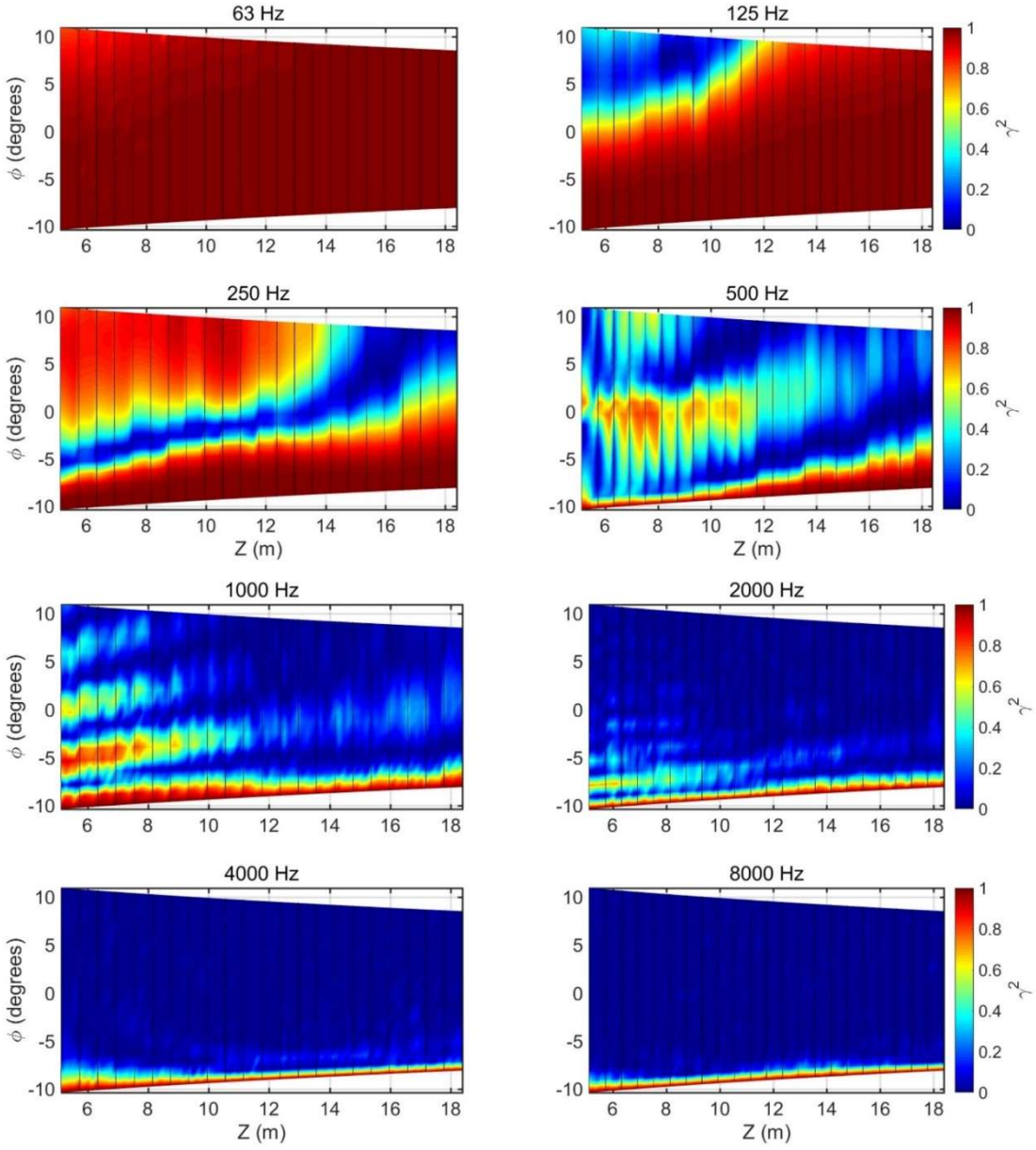

Figure 3 Coherence as a function of downstream distance for the octave band center frequencies between 63 and 8000 Hz. In each column of the measurement array, the coherence is calculated between each microphone and the microphone closest to the ground of that column. The array receded from the jet centerline at larger downstream distances so the angular coverage decreased.

Equation (1) yields $0 \leq \gamma^2 \leq 1$, where one signifies a perfectly linear transform between the two signals and zero means there is no relationship. A single acoustic source would produce a perfectly coherent field, with $\gamma^2 = 1$ between any two points, assuming there was no measurement noise or other nonlinearities in the system. In this study, the coherence was calculated for every pair of microphones in each column of the array.

To show trends in the coherence of the jet noise field as a function of frequency and space, Figure 3 contains plots of the coherence between the microphone closest to the ground and all the other microphones in that particular measurement column. Figure 3 reveals two issues with the attempt to obtain meaningful information from simply the calculation of the coherence. First, the aperture of this measurement was not large enough to encompass the entire source. Second, in comparing Figure 3 to the ground interference effects evident in Figure 2, reductions in coherence are caused by one of the microphones in a pair being located in a ground interference null. This effect is especially prominent at 125 and 250 Hz. At 1000 Hz as the array is scanned from bottom to top, the coherence drops in every interference null and increases again to a smaller maximum value, creating an envelope that decreases overall as angular separation increases. At 500 Hz, a unique effect occurs that yields an interesting physical insight for jet noise over a reflecting surface. Because the lowest microphone on the measurement array is actually inside the ground interference null, it is incoherent with the microphones within the regions of maximum radiation, however, the lowest microphone is surprisingly coherent with the other interference nulls higher on the array. This may mean a different coherent source phenomenon – one that is not cancelled by ground interference nulls at the same locations as the main radiation lobe – is present in the jet noise field.

Between the limitations of the measurement aperture and the interference of the ground reflection, looking at just the calculation of the coherence does not give a clear picture of source characteristics of interest. For this reason, a new quantity called the coherence angle, ϕ_{γ^2}, is defined as the maximum angle between two points where the coherence is above a value of 0.5 (similar to the coherence length used in Ref. 4, which was shown to be a figure of merit in Ref. 18). Absolute calculation of ϕ_{γ^2} at all frequencies is impossible as the array was of finite size and inter-element spacing. However, ϕ_{γ^2} can be given upper and lower limits as a function of z and frequency. When the calculated ϕ_{γ^2} is equal to the angular width of the entire array, it signifies that it is a minimum bound to the actual value for ϕ_{γ^2}. When the coherence angle is calculated to be zero, it means that the inter-element spacing in the array was larger than the actual ϕ_{γ^2}. The calculations of ϕ_{γ^2} can be summarized on a single plot as a function of frequency and z as shown in Figure 4. The horizontal axis of Figure 4 is the z-coordinate, the vertical axis is the narrowband frequency where the coherence was calculated, and the color corresponds to the value of ϕ_{γ^2} in degrees. The figure shows a clear trend in decreasing azimuthal coherence with increases in frequency and downstream distance. The black region of the figure is where the coherence angle was as large as or larger than the entire measurement aperture (and thus 23° serves as a lower limit to the actual value of ϕ_{γ^2} in this region) and the white region is where the coherence between neighboring microphones across the entire array was less than 0.5, so the angular resolution of the array is an upper bound to ϕ_{γ^2}.

Using the calculated ϕ_{γ^2} as an indicator of field coherence was effective at ignoring the influence of the ground interference nulls in most cases. An exception is when the ground reflection null at a single frequency was as large as the vertical span of a single measurement, so the angular coherence across multiple maxima could not be calculated, and the resulting ϕ_{γ^2}

between all positions measured are uncharacteristically low. Examples include bands centered on 125 Hz for $z < 12$ m, 200 Hz for $11 < z < 15$, and 250 Hz for $z > 14$. The data were ignored in these regions, which are marked as a brown patch superimposed on Figure 4.

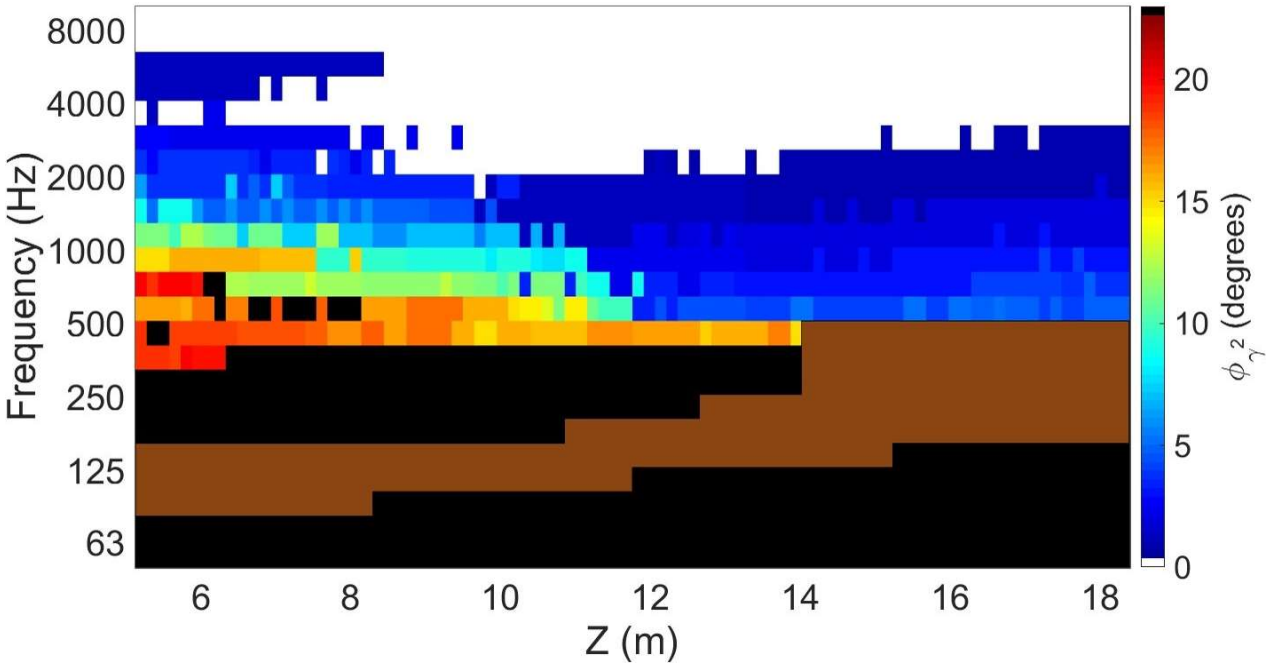

Figure 4 Coherence angle as a function of downstream distance and frequency. The black region is where the coherence angle was as least as large as the measurement aperture, the white area is where the coherence angle is smaller than the smallest microphone spacing in the array, and the brown region is where the entire vertical aperture was inside a ground reflection null so ϕ_{γ^2} could not be calculated reliably.

Other than the instances marked in brown, the trend is in agreement with general observations of laboratory scale jets.[12] Coherence angles are highly dependent on frequency, and only slightly dependent on downstream location by comparison. The black regions of Figure 4 show that frequencies below about 315 Hz have ϕ_{γ^2} values as high or higher than the minimum value of 20° dictated by the array aperture. Between 315 Hz and about 3150 Hz, coherence angle decreases with frequency, at which point the higher frequencies have coherence angles at or below about 1°, bounded by the microphone spacing. By extrapolation beyond the bounds, it can be hypothesized that the trends of coherence angle dependence on frequency continue outside the bandwidth of the data that can be shown here. A similar trend is seen in Harker et. al.[4] in Figure 12 b) that shows the axial coherence lengths for the same aircraft and engine power as investigated in this study. There, the axial coherence lengths rapidly decreased from being upwards of 4 m at 200 Hz to on the order of a meter at 500 Hz.

Inside the 500-2000 Hz region of Figure 4 that is not obscured by array limitations, the trends in ϕ_{γ^2} as a function of distance downstream offer additional insight. Overall, these data show that angular coherence decreases with distance downstream. This result may be surprising, given the well-supported theory that sideline noise is dominated by fine-scale, less-coherence radiation and the downstream region is dominated by highly coherent waves produced by large-scale turbulence structures. As before, the key to this apparent discrepancy lies in the spatial bounds of the array, this time in the axial direction. Figure 2 showed that between 500 Hz and 2000 Hz, the highest 10-dB amplitude regions are restricted to z<12 m, the same regions where the highest ϕ_{γ^2} values

occur in Figure 4. Thus, high coherence values tend to be collocated with high levels, consistent with the idea that maximum jet noise radiation comes from the most coherent turbulent sources. Farther aft of $z = 12$, the drop in angular coherence provides further support that there is significant source information of relatively low coherence radiating in all directions (not just to the sideline) that is masked by the main radiation lobes in the high-amplitude region but emerges clearly away from these regions, both downstream and in the nulls of the interference pattern as discussed above.

C. M-SONAH Reconstruction

Since high field coherence implies a single, self-coherent source, if the field is to be decomposed into mutually orthogonal azimuthal modes, a single one should be sufficient to reconstruct the field over the measurement aperture where the coherence is high. To test if a single azimuthal mode is sufficient to reconstruct the salient features of a jet noise field with large ϕ_{γ^2}, an advanced method of near-field acoustical holography (NAH) known as multisource statistically optimized NAH (M-SONAH) is employed to reconstruct the pressure field at locations measured by the vertical scan array. This was done by using a measurement taken from a measurement plane similar in extent to the vertical scans but at a different location, then applying the algorithm to reconstruct the field at the vertical scan locations. The details of the formulation for this algorithm are found in Refs. 17 and 19. For this study, some axisymmetry is imposed on the problem because the addition or inclusion of any more than the zeroth-order Hankel function in the NAH equivalent wave model did not improve the reconstruction accuracy.[19]

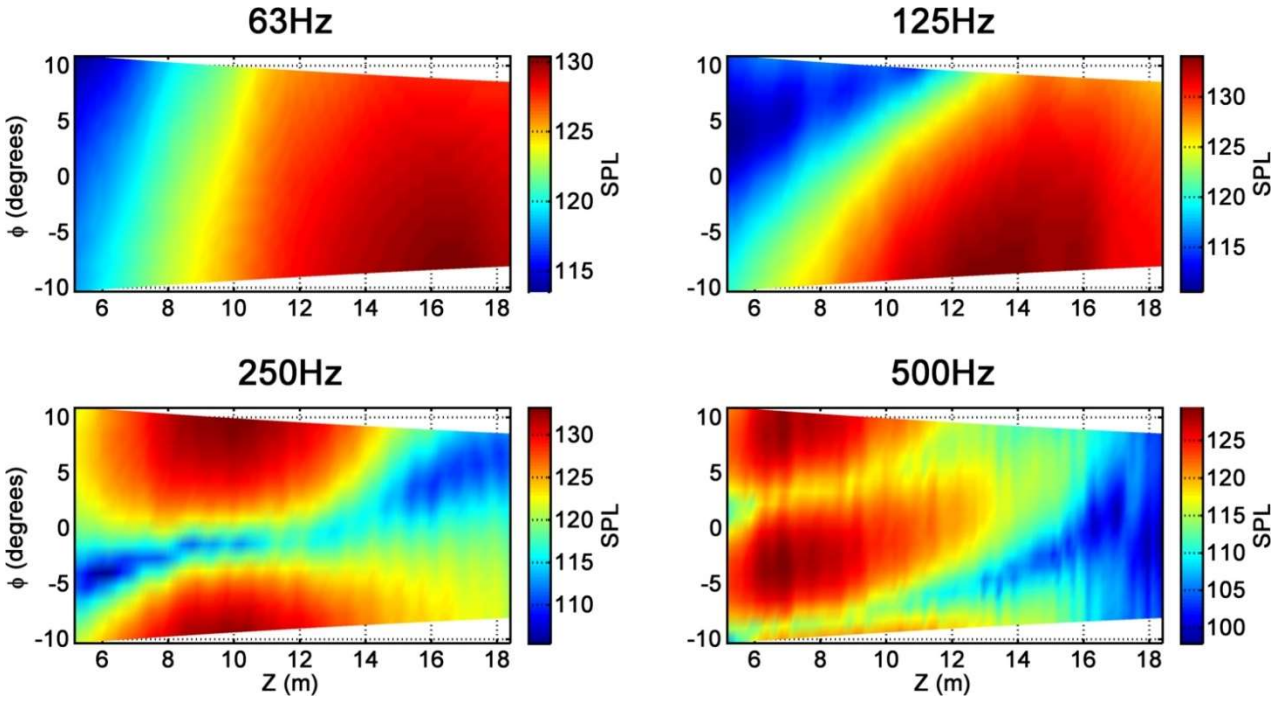

Figure 5 The sound pressure levels of the M-SONAH reconstruction on the measurement aperture for 63, 125, 250, and 500 Hz.

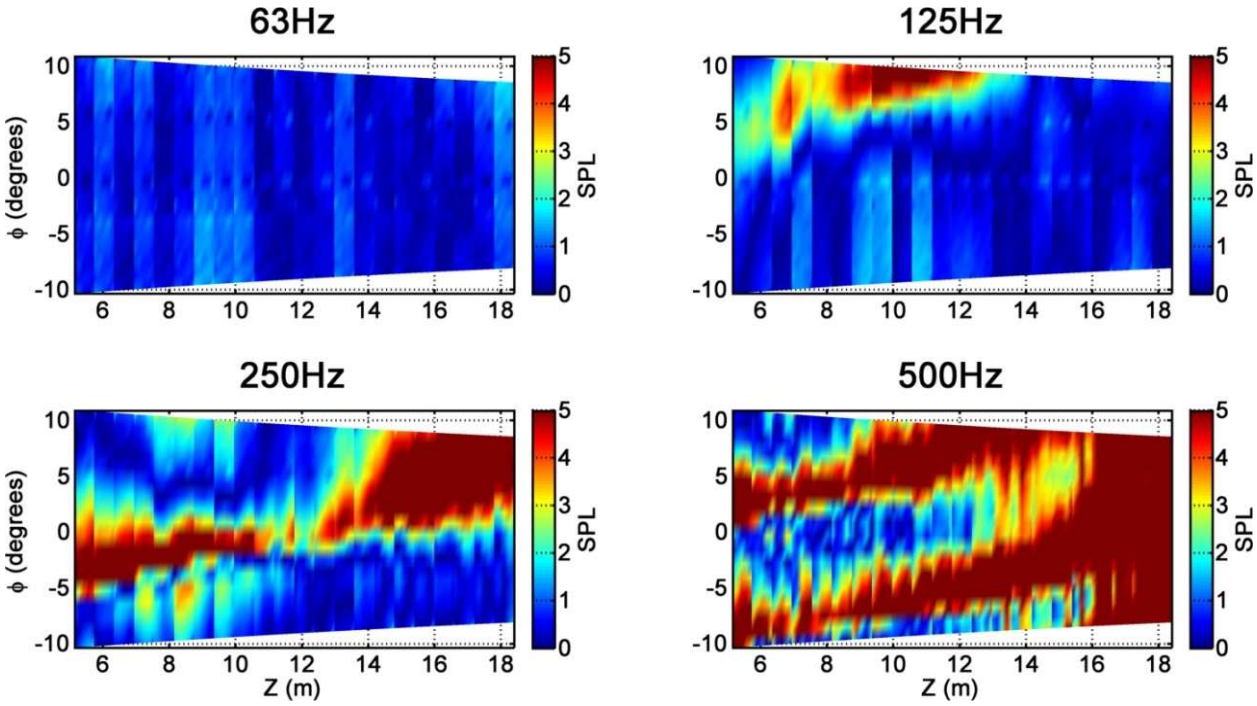

Figure 6 The absolute value of the difference between the measured data (Figure 2) and the M-SONAH reconstruction (Figure 5).

The validity of the M-SONAH method is confirmed for 63-500 Hz by comparing the SPL of the reconstructions to the measured levels. Figure 5 shows the levels of the reconstruction and Figure 6 shows the difference between the reconstructions and the measurement. It is seen that there is excellent agreement in the shape and level of the reconstruction, with the exception of the null regions where the M-SONAH algorithm underestimates the level. The underestimation of the levels in the null regions by M-SONAH is believed to be due to its ideal nature, where the actual measurements contain consequences of the real world environment such as the effects of atmospheric turbulence and the fact that the source is turbulent and volumetric[20].

The spatial coherence of the M-SONAH reconstructed field is calculated for each column with reference to the lowest microphone and displayed in Figure 7 in the same manner as the measured coherence in Figure 3. For all four frequencies, the reconstructed locations of coherence maxima and null regions are in good agreement with those of the measurements. Accurate spatial sound field mapping of field levels was shown to be a strength of NAH methods in Figure 6 and in past investigations,[19] and Figure 7 demonstrates that coherence maps can also be reproduced with high spatial precision. In regards to magnitude accuracy, note that the predicted coherence values at all frequencies in Figure 7 tend to be higher than the measured values, with the worst-case overpredictions at 500 Hz. Both the partial field decomposition and the SONAH algorithms employ singular-value decompositions and regularization to remove measurement noise (avoiding problems with the inversions of ill-posed matrices), and the result is that some low-amplitude sound source information is removed as well. The interesting result is that, while this tends to give underpredictions of field levels (see Figure 6), it results in the overpredictions of coherence seen here in Figure 7. Even so, the spatial coherence of jet noise fields cannot be represented at all, even with the best level-based models, unless multiple mutually incoherent source terms are

included or the coherence is included explicitly. NAH is one such method, and it is demonstrated as a feasible coherence modeling tool in a challenging acoustic environment.

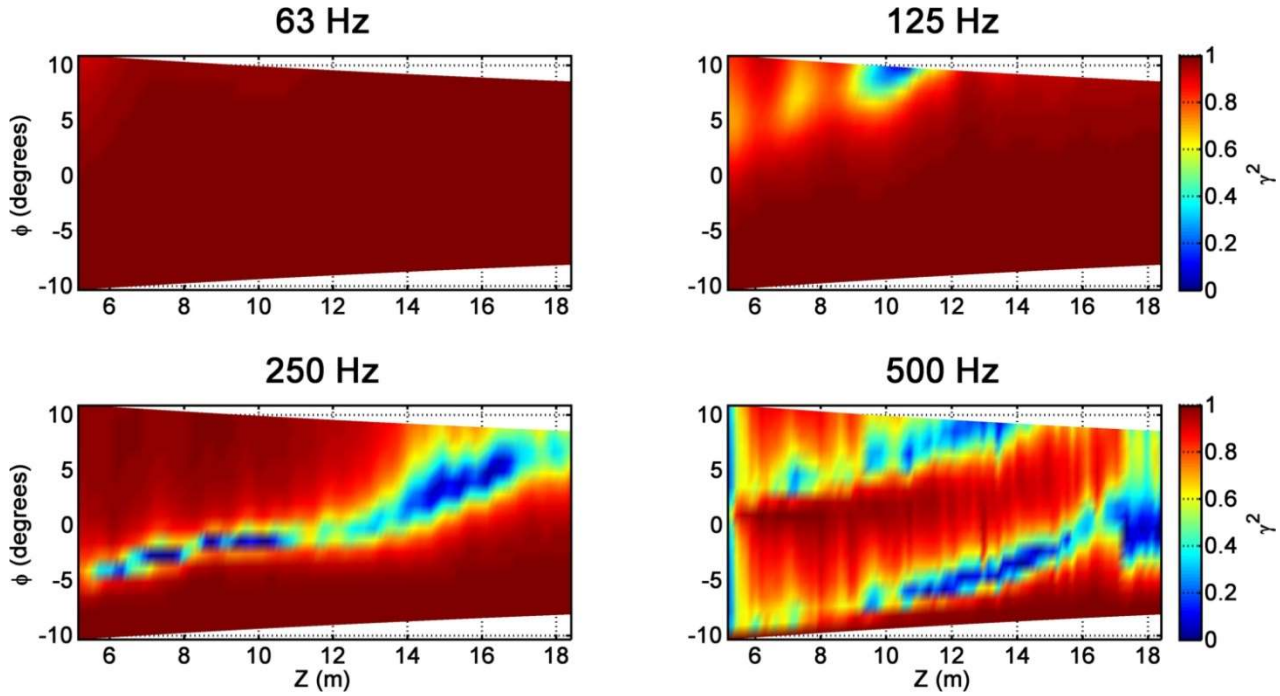

Figure 7 The azimuthal coherence of the M-SONAH reconstruction along the measurement array for 63, 125, 250, and 500 Hz. Similar to Figure 3, the coherence is shown by relating each microphone to the lowest microphone in the array for each downstream distance.

3. CONCLUSIONS

Bounds on the coherence angles, ϕ_{γ^2}, around the axis of the jet plume of a high-performance military aircraft have been calculated. Coherence angle values are at least as large as 20° for all frequencies below 315 Hz for all measured downstream distances. As frequency increases, ϕ_{γ^2} decreases to less than 1° by 3150 Hz. The highest azimuthal coherence values tend to occur in the regions of maximum radiation levels, consistent with the idea that the strongest sources are produced by highly coherent turbulent structures. However, away from these strong radiation lobes (e.g. far downstream and in the null regions of the strong interference patterns from the ground reflection), low-amplitude, low-coherence information is prevalent, suggesting the presence of additional source information that is distinct from (and hidden under) the main radiation. This is hypothesized to be, at least in part, due to fine-scale turbulence that radiates in all directions, not just to the sideline where it dominates. This theory is supported by the work of Neilsen et al.[21], who showed the presence of spectral content matching that of the theoretical fine-scale spectrum curve downstream of the main radiation lobe. The low-amplitude jet noise sources could be investigated further through the use of partial field decomposition methods that rely on spatial coherence inputs.[22]

Additionally, an unexpected phenomenon is observed where the measurements taken in multiple ground interference nulls at a single frequency are coherent with each other, and incoherent with the measurements of the lobes. This could suggest that there are multiple, spatially distinct sources in the plume which therefore have different ground reflection patterns, so when

one is experiencing an interference null the other is not, effectively giving an opportunity to probe the field caused by different sources.

In the second portion of this paper, it was shown that NAH reconstructions of the sound field produced high-fidelity predictions of both amplitude and azimuthal coherence, although the NAH noise-filtering processes caused some underpredictions of level and overpredictions of coherence. Overall, the NAH methods developed for full-scale jet noise investigations were shown here to be a viable option for full-field radiation modeling, and the ability to reproduce field coherence will assist investigations of multiple sources that can be targeted for noise reduction efforts.

Though this study was limited by the angular aperture of the array, it is important to note that it covers the region where personnel would be present in many military aircraft contexts such as run-up pads or aircraft carriers.

ACKNOWLEDGMENTS

This research was supported in part by an appointment of Kevin Leete to the Student Research Participation Program at the U.S. Air Force Research Laboratory (USAFRL), 711th Human Performance Wing, Airman Systems Directorate, Warfighter Interface division, Battlespace Acoustics Branch administered by the Oak Ridge Institute for Science and Education through an interagency agreement between the U.S. Department of Energy and USAFRL. Funding for the Measurements was provided by USAFRL through the Small Business Innovation Research program, and supported through a cooperative research development agreement between Blue Ridge Research and Consulting, Brigham Young University, and the U.S. Air Force. Additional funding for this analysis was provided by the Office of Naval Research.

Distribution statement A. Approved for public release: distribution is unlimited. 88ABW Cleared 01/10/18; 88ABW-2018-0099

REFERENCES

[1] C. K. Tam, K. Viswanathan, K. K. Ahuja and J. Panda. "The sources of jet noise: experimental evidence", J. Fluid Mech. **615**, 253-292 (2008).

[2] C. K. W. Tam, M. Golebiowski, J. M. Seiner, "On the Two Components of Turbulent Mixing Noise from Supersonic Jets", AIAA paper 96-1716, (1996)

[3] L. Ukeiley and M. Ponton, "On the Near Field Pressure of a Transonic Axisymmetric Jet," Intl. J. Aeroacoustics, **3**, 43-66 (2004).

[4] B. M. Harker, T. B. Neilsen, K. L. Gee, A. T. Wall and M. M. James, "Spatiotemporal-Correlation Analysis of Jet Noise from a High-Performance Military Aircraft," AIAA Journal, **54**, 1554-1566 (2016)

[5] C.E. Tinney and P. Jordan, "The near pressure field of co-axial subsonic jets," J. Fluid Mech., **611**, 175-204 (2008).

[6] R. E. A. Arndt, D. F. Long, M. N. Glauser, "The proper orthogonal decomposition of pressure fluctuations surrounding a turbulent jet" J. Fluid Mech. **340,** 1-33 (1997).

[7] D. Papamoschou "Wavepacket Modeling of the Jet Noise Source" 17th AIAA/CEAS Aeroacoustics Conference (32nd AIAA Aeroacoustics Conference). Portland, Oregon (2011).

[8] H. Vold, P. Shah, P. Morris, Y. Du and D. Papamoschou, "Axisymmetry and azimuthal modes in jet noise", 18th AIAA/CEAS Aeroacoustics Conference (33rd AIAA Aeroacoustics Conference), Colorado Springs, CO (2012)

[9] B. M. Harker, K. L. Gee, T. B. Neilsen, A.T. Wall, M. M. James, "Wavepacket Modeling and Full-scale Military Jet noise Beamforming Analyses," 54th AIAA Aerospace Sciences Meeting, AIAA SciTech, (2016).

[10] T. B. Neilsen, K. L. Gee, B. M. Harker, M. M. James, "Level –educed Wavepacket Representation of Noise Radiation from a High-Performance Military Aircraft," 54th AIAA Aerospace Sciences Meeting, AIAA SciTech (2016).

[11] Tracianne B. Neilsen, Aaron B. Vaughn, Kent L. Gee, Masahito Akamine, Koji Okamoto, Susumu Teramoto, Seiji Tsutsumi, "Level-educed Wavepacket Represenation of Mach 1.8 Laboratory-Scale Jet Noise", AIAA Paper 2017-4049 (2017).

[12] K. Viswanathan, J. R. Underbrink and L. Brusniak, "Space-Time Correlation Measurements in Near Fields of Jets," AIAA Journal **49**, No. 8, 1577-1599 (2011).

[13] A. V. G. Cavalieri, P. Jordan, T. Colonius and Y. Gervais, "Axisymmetric superdirectivity in subsonic jets," J. Fluid Mech. **704**, 388-420 (2012).

[14] C. A. Brown and J. Bridges, "Acoustic Efficiency of Azimuthal Modes in Jet Noise Using Chevron Nozzles," 12th AIAA/CAES Aeroacoustics Conference (27th AIAA Aeroacoustics Conferrence), Cambridge, Massachusetts (2006).

[15] H. V. Fuchs and U. Michel "Experimental Evidence of Turbulent Source Coherence Affecting Jet Noise," AIAA Journal, **16**, No. 9, 871-872 (1978).

[16] A. T. Wall, K. L. Gee, M. M. James, K. A. Bradley, S. A. McInerny and T. B. Neilsen, "Near-field noise measurements of a high-performance military jet aircraft," Noise Control Eng. J. **60**, 421-434 (2012).

[17] A. T. Wall, K. L. Gee and T. B. Neilsen, "Multisource statistically optimized near-field acoustical holography" J. Acoust. Soc. Am. **137**, 963-975 (2015).

[18] A.T. Wall, M. D. Gardner, K. L. Gee, and T. B. Neilsen, " Coherence length as a figure of merit in multirefrence near field acoustical holography" J. Acoust. Soc. Am. **131** 2422-2430 (2012)

[19] A. T. Wall, K. L. Gee, T. B. Neilsen, R. L. McKinley, and M. M. James, "Military jet noise source imaging using multisource statistically optimized near-field acoustical holography," J. Acous. Soc. Am. **139**, 1938 (2016)

[20] K. L. Gee, T. B. Neilsen, and M. M. James, "Including source correlation and atmospheric turbulence in a ground reflection model for rocket noise," Proc. Mtgs. Acoust. **22**, 040001 (2014)

[21] T. B. Neilsen, K. L. Gee, A. T. Wall, and M. M. James, "Similarity spectra analysis of high-performance jet aircraft noise," J. Acoust. Soc. Am. 133, 2116-2125 (2013)

[22] A. T. Wall, K. L. Gee, K. M. Leete, T. B. Neilsen, T. A. Stout, and M. M. James, "Partial-field decomposition analysis of full-scale supersonic jet noise using optimized-location virtual references," J. Acoust. Soc. Am. (submitted 2017).